# Investigating the Anti-cancer Activity of Novel Michael Acceptors

BY

Alexander J. Hack-Polay

A thesis submitted to the

Department of Biology

Mount Allison University

In partial fulfillment of the requirements for the

Bachelor of Science degree with Honours

April 9, 2024

Table of Contents

**Acknowledgements**

I would like to thank Dr Andrew Grant for his guidance and support throughout this Honour's project. Being able to work under and learn from such a knowledgeable and passionate chemist has allowed me greatly to broaden my interdisciplinary knowledge through this project. I am grateful to have had the opportunity to be part of such a novel and exciting project.

I would also like to thank Dr Jillian Rourke, whom without, this project would not have been possible her extensive generosity in providing the lab space, equipment, and cells to work with. Furthermore, her mentorship from the biochemistry/biology standpoint was critical to the success of this project.

Thank you to all of the Rourke Lab members: Aditaya Kalia, Logan Reid, Megan Campbell, Isaac McCardle, Sun Min Park and Tyler Lutes. I highly appreciate your advice and sharing the lab space throughout this project.

Thank you to the Grant Lab members: Spencer Scott, Tiana Sharpe, Anas Iqelan. I extend a special thank you to Tiana Sharpe whose role in synthesizing the novel Michael acceptor compounds laid the foundation for my research project. Her help in understanding the complex chemistry at work was highly appreciated.

Finally, I also thank everyone who has been part of my incredible support system during this long journey with many ups and downs. Particularly I thank Brooke Fredericks for being my biggest supporter, spending many late nights with me as I work odd and long hours, and for encouraging me to keep going even during the hardest periods. I also extend thanks my friend Samuel Bujold for always being willing to be a listening ear.

**Abstract**

Cancer, in its multiple forms, remains a major health concern globally. Tremendous effort is expended annually by the pharmaceutical industry and academia to understand cancer, and develop new treatments. Chronic lymphocytic leukemia (CLL) is of particular interest to this lab. A drug that treats CLL with great effectiveness is Ibrutinib. This drug belongs to a class of compounds known as Michael acceptor compounds (MACs). MACs are able to form powerful covalent bonds with a variety of biological targets. To that end, several novel Michael acceptors have been synthesized in the Grant Lab. This study investigated the cytotoxicity of these novel Michael acceptors against HCT116 colon cancer cells as well as investigated the cell death pathway induced by these compounds. The MTT assay and cell count were used to measure cell viability after exposure to the compounds. Further, Brightfield of the cells and fluorescent images of the nuclei were examined to begin to elucidate cell death pathway. The results of this study found that the novel MACs were able to have a measurable cytotoxic effect on HCT116 cells. The morphological analysis suggests that the novel MACs induce the necrosis cell death pathway in these cells although future biochemical methods will be needed to confirm this result.

## List of Tables

## List of Figures

## List of Abbreviations

ANOVA – Analysis of Variance

CR – Cell rounding

DMEM - Dulbecco's modified eagle medium

DMSO – Dimethyl sulfoxide

EWG – Electron withdrawing group

FBS - Fetal bovine serum

IEI – Irreversible enzyme covalent inhibitor

MAC – Michael acceptor compound

MAF – Michael acceptor functional group

MAR – Michael addition reaction

MD – Michael donor

MR – Membrane rupture

MTT – (3-(4,5-dimethylthiazol-2-yl)-2,5-diphenyltetrazolium bromide)

NFA – Nitro fatty acid

PBS – Phosphate buffered saline

PK – Pyknosis

SEM – Standard error of the mean

# 1. Introduction

## 1.1 Rise of Michael acceptor drugs

Discovering new drugs is a constant challenge in the pharmaceutical industry. Recently, Michael acceptor drugs have become very attractive candidates. Despite having a high level of bioactivity and potential reactivity with a vast number of cellular components and systems, the full potential of compounds with a Michael acceptor functional group (MAF) has not been exploited due to their lack of selectivity (Piesche et al., 2020). More recently, pharmacological research groups have revised this stance on Michael acceptor compounds (MACs) and have begun investigating to elucidate their mechanism of action in order to exploit them in a manner that allows for selective targeting (Jackson et al., 2017). This has resulted in the emergence of ground-breaking drugs such as Ibrutinib, Afatanib, and Osimertinib (Jackson et al., 2017). The ability of MACs to act as powerful covalent inhibitors can aid in overcoming drug resistance (Jackson et al., 2017). This important attribute warrants further investigation and screening of MACs (Jackson et al., 2017).

MACs are used to treat a wide range of diseases and dysfunctions, including MACs that act as anti-inflammatory and anti-cancer agents (Piesche et al., 2020). Nitro fatty acids (NFAs) are endogenously produced MACs that provide inspiration for the use of MACs in the treatment of cardiovascular disease (Piesche et al., 2020). NFAs are a product of the metabolism of fatty acids during inflammation (Villacorta et al., 2016). Evidence shows that NFAs are partially responsible for cardio protection via a variety of anti-inflammatory mechanisms often involving a Michael addition reaction (MAR) – unique to MACs (Villacorta et al., 2016). For example, NFAs may bind to 5-lipoxygenase to inhibit its activity, consequently promoting production of anti-inflammatory eicosanoids (Villacorta et al., 2016).

### 1.2 What are Michael acceptor compounds/ What is the Michael addition reaction?

Arthur Michael discovered the Michael Addition reaction (MAR) in 1887. He discovered a unique reaction between compounds containing an α,β-unsaturated bond paired with an electron withdrawing group (EWG), usually a carbonyl, called MACs and a nucleophile called an Michael donor (MD) (Liang et al., 2022). Some of the most common biological MDs are amines and thiols, which are abundant in the composition of proteins and other small biomolecules (Hearn et al., 2021). The β-carbon of the MAC is made to be electron deficient due to the pull on electrons towards the EWG. This makes the β-carbon the preferred site of attack for a nucleophile MD which attacks the β-carbon and donates an electron pair to form a strong bond. The carbon's maximum capacity of four valence electrons is exceeded so when the MD binds, the electrons on the double bond move all the way to the electronegative oxygen, forming and "enolate", which eventually quenches by attaching a proton ($H^+$) to the α-carbon. This forms a covalent bond.

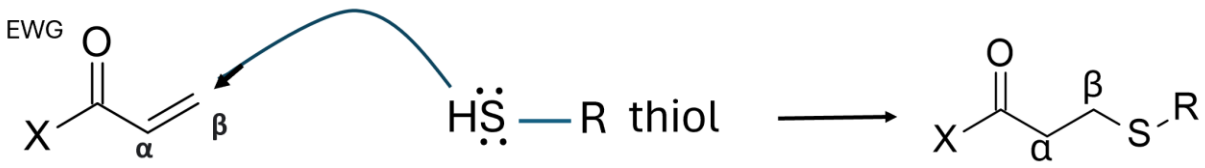


**Figure 1**. **Simplified diagram of the Michael addition reaction.** Diagram created on BIOVIA draw.

### 1.3 CLL and Ibrutinib mechanism of action

Chronic lymphocytic leukemia (CLL) is another devastating disease for which MACs have been instrumental in treatment. CLL is the most common type of leukemia in the Western world. It is a cancer in which there is an overaccumulation of B-cell white blood cells (B-lymphocytes) in peripheral bone marrow, the lymph nodes, and the spleen (Ghia et al., 2007). CLL and other B-cell cancers can often arise from aberrant B-cell receptor

signalling (Arnason & Brown, 2017). The aforementioned revolutionary drug Ibrutinib, is used to treat these cancers.

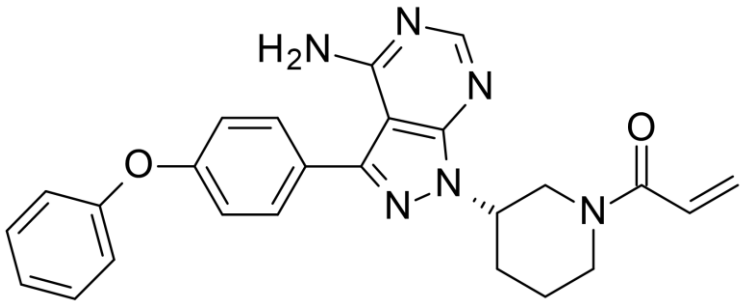


**Ibrutinib.** Diagram created on BIOVIA draw.

This anticancer drug targets Bruton's tyrosine kinase (BTK) which is part of the B-cell receptor (BCR) signalling pathway (Arnason & Brown, 2017). The BCR signaling pathway is activated when an antigen stimulates BCR leading to the recruitment of transmembrane peptides CD79a and CD79b and subsequent activation of spleen tyrosine kinase and LYN kinase (Arnason and Brown, 2017; Wu et al., 2019). Next in the pathway immunoreceptor tyrosine-based activation motifs (ITAMs) are phosphorylated by SYK and LYN (Arnason & Brown, 2017). This cascade leads to the activation of BTK that carries out the phosphorylation of downstream targets leading to the release of calcium stores and upregulation of transcription factors that are implicated in migration, proliferation, and other survival processes of B-cells (Arnason & Brown, 2017).

Due to its crucial role in B-cell cancers' pathogenesis, the BCR signalling pathway is a common therapeutic target (Burger & Chiorazzi, 2013). BTK is one of the preferred targets in the pathway as it's downstream position allows for concentrated therapeutic development whereas attempts to disrupt antigen binding or antigen deprivation would be more difficult given the antigen binding promiscuity of BCRs (Burger & Chiorazzi, 2013). Ibrutinib undergoes a MAR with cysteine C481 in the BTK active site, blocking ATP from binding and thus inhibits BTK's kinase activity (Zhou et al., 2020). This in turn inhibits its ability to complete its role in the BCR signalling pathway, ultimately reducing proliferation and survival of pathogenic B-cells (Zhou et al., 2020).

## 1.4 Reversible vs irreversible inhibitors - 2 Distinct classes of compounds

### *1.4.1 Disadvantages of irreversible enzyme inhibitors*

Irreversible enzyme inhibitors (IEIs) are molecules that irreversibly inhibit enzyme activity, often by binding strongly to the active site, permanently preventing the enzyme from acting on any other substrate (Walpole & Wrigglesworth, 1989). Other irreversible inhibitors may work by allosterically binding to the enzyme and modulating it in such a way that it can no longer act on its substrate despite the active site remaining open (Rando, 1975). Irreversible inhibitors have long been approached with hesitation due to several hurdles they present, another reason for the slow adoption of MACs in the development of drug treatments (González-Bello, 2016).

Despite the history of skepticism surrounding irreversible inhibitors some of the most commonly administered drugs are irreversible inhibitors such as aspirin and penicillin (González-Bello, 2016). One of the main complications with the use of irreversible inhibitors is the generation of an immune response to the protein adducts that can be formed when the drug, or its metabolite, covalently binds with the enzyme (Johnson et al., 2010). A protein adduct is a complex of the protein (enzyme) and drug (Johnson et al., 2010). It is theorized that the complex is no longer recognized as endogenous and can act as an antigen for the immune system (Johnson et al., 2010). This is thought to be the origin of some “idiosyncratic” adverse reactions to drugs that are irreversible enzyme inhibitors (Johnson et al., 2010). There is no clear pattern that can be followed to determine when a drug-protein adduct will be immune aggravating so when irreversible enzyme inhibitor drugs are being developed, researchers take several preventative steps (Evans et al., 2004).

During drug development scientists strive to design the drug in a way that minimizes the formation of metabolites that may be highly reactive (Evans et al., 2004). One of these methods is the use of small molecule trapping agents (Evans et al., 2004). Molecular trapping agents are molecules such as glutathione that can form stable adducts with the reactive metabolites if present (Evans et al., 2004). Because they work well with liquid chromatography-tandem mass spectrometry they are very useful in screening for

bioreactivity of metabolites formed from trial drugs applied in vivo or in vitro (Evans et al., 2004).

IEIs are not desirable when treatment requires a short-lived interaction with the target enzyme or partial inhibition (Johnson et al., 2010). In other words, there are some therapeutic targets for which it would be inappropriate to permanently inactivate them (Johnson et al., 2010). For example, IEIs should not be used to reduce excessive signalling from critical receptors as a complete block of their function can lead to extreme side effects (Johnson et al., 2010).

Selectivity is of course a heightened concern when considering the development and use of IEIs. They pose a greater risk of toxicity if insufficiently selective due to the permanent nature of their binding with targets (Boike et al., 2022). Thus, the drug must maintain a high level of selectivity and well balanced reactivity to reduce interaction with off-target proteins but still sufficiently bond with the target enzyme (Boike et al., 2022).

### *1.4.2 Advantages of irreversible enzyme inhibitors*

In contrast, there are many advantages to IEIs that make them desirable drug candidates and often an ideal solution. IEIs require reduced dosing compared to reversible enzyme inhibitors due to their potent toxicity (Sutanto et al., 2020). This toxicity partially occurs as a result of their long target binding time. Data shows that patients are more likely to adequately follow instructions for drugs that require reduced dosing i.e. prescribed to be taken less frequently (Sutanto et al., 2020). IEIs also provide the added benefit of being able to overcome resistance mechanisms that can develop with drug treatment (Sutanto et al., 2020).

To further elaborate, the reasons lower doses of IEIs are required are because they permanently inactivate the target meaning that for the target to have a significant effect again it needs to be resynthesized by the body (Johnson et al., 2010). This allows a longer period of time during which the drug doesn't need to be administered – even when the drug is not detected in the blood, the effect lasts (Johnson et al., 2010). Further supporting

this effect, because the drug permanently binds, it does not need to keep competing with endogenous ligands (~80% of available drugs compete with endogenous ligands) so lower levels need to be maintained in the body (Johnson et al., 2010).

IEIs have been seen to be capable of overcoming resistance. An example of this is seen in the targeting of epidermal growth factor receptor (EGFR) in cancers (Michalczyk et al., 2008). EGFRs are involved in mediating cell proliferation, a mutation in EGFRs can lead to uncontrolled cell proliferation and consequently cancer, thus they are a common target for anti-cancer drugs (Michalczyk et al., 2008). However, EGFRs are also capable of developing a mutation where a methionine is coded for rather than a threonine at an important location such that ATP competitive inhibitors can no longer bind (Michalczyk et al., 2008). IEIs such as a 4-(phenylamino)quinoline group are able to overcome this resistance due to the longer time spent in the active site which allows a Michael addition to occur (Michalczyk et al., 2008). This reaction shifts the equilibrium in favour of the drug staying bound even with the binding site being less favourable for it (Michalczyk et al., 2008).

## 1.5 Investigating cytotoxicity

### *1.5.1 Assessing cytotoxicity via cell viability*

The MTT (3-(4,5-dimethylthiazol-2-yl)-2,5-diphenyltetrazolium bromide) assay is used by almost all studies investigating cytotoxicity (Ghasemi et al., 2021). The MTT assay takes advantage of cells' automatic reduction of the MTT reagent into purple formazan crystals in the mitochondria while alive (Riss et al., 2004). The end result of the MTT assay provides a colorimetric representation of the proportion of cells alive following treatment (Riss et al., 2004).

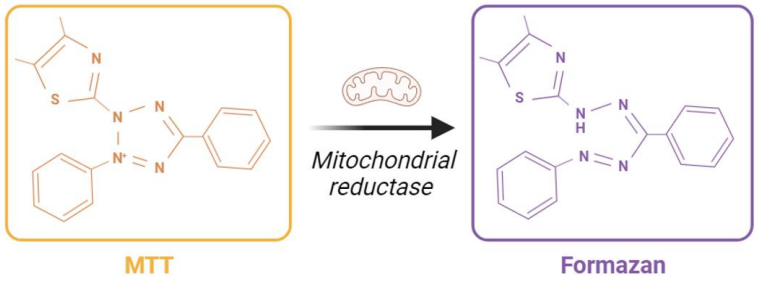


**Figure 2. Yellow MTT reagent is converted to purple formazan crystals in the mitochondria.** Figure adapted from Biorender.com

### *1.5.2 Morphologically distinct cell death pathways*

The three most common morphologically distinct types of cell death are apoptosis, autophagic cell death, and necrosis (Green & Llambi, 2015).

Apoptosis, also referred to as Type I cell death, is characterized by the shrinking of cells into a particularly round shape while maintaining an intact plasma membrane accompanied by condensation of chromatin and nucleus fragmentation (Kroemer et al., 2005). The cell adopts a rounded shape because it severs connections to other cells as it dies (Häcker, 2000). These features can be visualized under light microscopy. Nuclear staining allows for the chromatin condensation and nuclear fragmentation (karyorrhexis) to be visualized (Häcker, 2000). The apoptosis cell death pathway is governed by caspases (cysteine proteases) (Yuan et al., 1993).

Autophagic cell death is also referred to as Type II cell death (Shimizu et al., 2014). Autophagic cell death is best visualized using electron microscopy as the morphological characteristics that distinguish it are on the level of the organelle (Kroemer et al., 2005) These include the formation of autophagic vacuoles in the cytoplasm that can be distinguished from other types of vesicles when using this level or resolution (Kroemer et al., 2005). Autophagy is a process used by cells to maintain an optimally functioning intracellular environment by removing and recycling damaged organelles (Miller &

Zachary, 2017). Autophagy can be used by cells to avoid apoptosis but will promote cell death if it degrades an inhibitor of caspase activity (Yonekawa & Thorburn, 2013).

Necrosis (Type III cell death) is often thought of as more of an "accidental cell death" in comparison to apoptosis (Kroemer et al., 2005). Some hallmarks of necrosis can be identified with light microscopy, these include pyknosis, karyorrhexis, and karyolysis (Miller & Zachary, 2017). Pyknosis is nuclear condensation and karyolysis is the loss of the nucleus (Miller & Zachary, 2017). Perhaps the most distinctive sign of necrosis is the ruptured plasma membrane (Leist et al., 1997). During necrosis the cell and organelles within increase in volume to the point of plasma membrane rupture (Kroemer et al., 2009). Necroptosis is a more controlled form of necrotic cell death that has similar morphological features to necrosis (Berghe et al., 2010).

The cell death pathway initiated by a drug is of interest in pharmacology because cancers can resist or evade apoptosis and thus triggering alternative forms of cell death is advantageous (Hanahan & Weinberg, 2011). Leakage of contents into the extracellular environment during necrotic cell death can trigger an immune response against cancer cells in vivo (Krysko et al., 2017).

### 1.6 Purpose of Investigation

This thesis explores the anti-cancer activity of a novel Michael acceptor functional group synthesized in the Grant lab at Mount Allison University. Specifically, this study investigates the cytotoxicity induced on human colon cancer cells (HCT116) by MACs with a novel MAF. Cell morphology will also be assessed in an attempt to elucidate the cell death pathway induced. Given the high reactivity of MACs with biomolecules we hypothesize that the MACs will have measurable cytotoxicity against HCT116 cells which will vary depending on the molecular structure.

The development of the novel MACs in the Grant lab came about in the following way. The Grant lab had been studying the Enone for several years. Tiana Sharpe (a chemistry Honours student) showed that the Enone behaved chemically as a Michael

acceptor. Being aware of the chemical structure of Ibrutinib (his sister had taken it for the treatment of CLL several years earlier), Grant saw the resemblance between the α,β-unsaturated nature of the Enone and the Michael acceptor portion of Ibrutinib. He wondered if he couldn't replace the Michael acceptor on Ibrutinib with a 5-membered ring version that contains sulfur in the ring as shown (a dihydrothiophene ring), a ring system he was certain he could synthesize. Knowing that Ibrutinib is synthesized from acryloyl chloride and the corresponding cyclic amine, all that was required was to synthesize the corresponding dihydrothiophene ring-containing acid chloride shown. Tiana Sharpe was able to synthesize this simple, but previously unknown molecule, in the spring of 2023. HP3, HP4 and HP5 were synthesized from the acid chloride as shown.

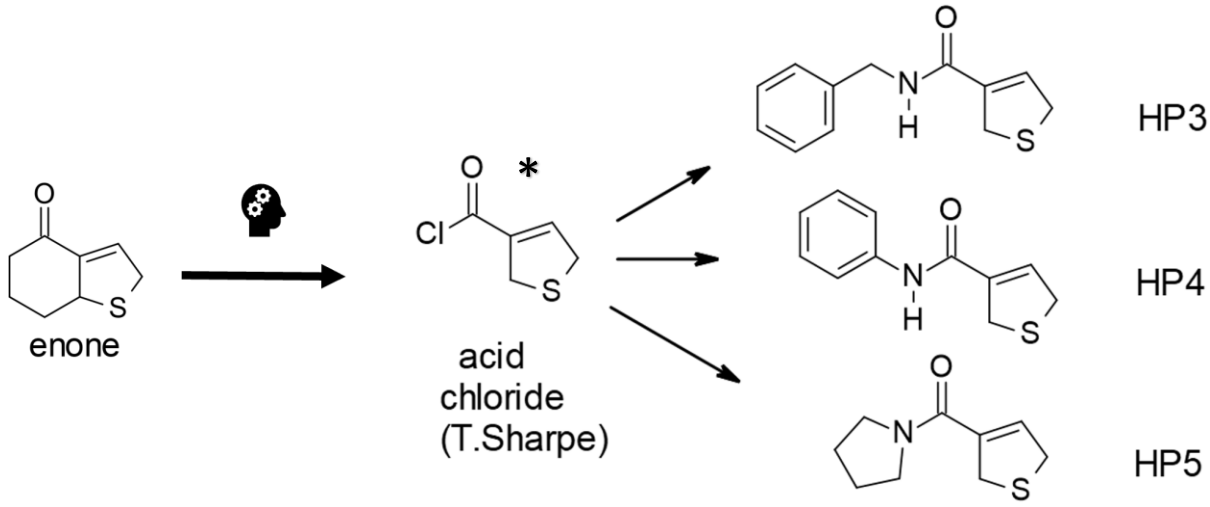


**Figure 3. Rational behind synthesis of the novel MAF (denoted by *) and attachment to back bone molecules to form final experimental MACs.** Diagram drawn in BIOVIA draw.

## 2. Methods

### 2.1 Human cell culture

Colon cancer cells (HCT116) were used for all toxicity testing – generously provided by the Rourke lab at Mount Allison University. Cells were cultured in Dulbecco's Modified Eagle Medium (DMEM; Corning 10-013-CV) supplemented with 10% fetal bovine serum (FBS; Corning 25-077-CV) (complete DMEM). Cells were grown in 10 cm tissue culture plates and routinely passaged after ~ 3 days when they reached ~70% confluency. To passage, the 10cm tissue culture plate with the cell colony was washed with 5 ml 1 X phosphate buffered saline (PBS) followed by trypsinization with 500 µL 0.25% Trypsin /2.21 mM ethylenediaminetetraacetic acid (EDTA; Corning 25-053-CI) and incubation for 4 minutes at 37°C and 5% $CO_2$. Cells were then collected from the plate with a 4.5 ml wash using complete DMEM and centrifuged for 5 minutes at 500 rcf. Supernatant was then removed and cells were resuspended in complete DMEM. The solution of cells was diluted 1:10 and plated in a 10 cm tissue culture plate.

### 2.2 Stock solution preparation of experimental and control compounds

All of the experimental Michael Acceptor compounds used were designed and synthesized in the Grant Lab at Mount Allison University by Dr Andrew Grant and Tiana Sharpe.

#### *2.2.1 Water-soluble experimental compounds – Enone, HP1, HP2, and HP5*

The compounds coded Enone, HP1, HP2, and HP5 were sufficiently water soluble and consequently each was dissolved in MilliQ purified $H_2O$ to create a stock concentration of 10,000 µM. There was an additional compound coded HP4 however issues with synthesis meant that it was not suitable for biological testing.

### *2.2.2 Non-water-soluble experimental compound – HP3*

The compound coded HP3 was found to not be sufficiently water soluble. This compound was dissolved in Dimethyl Sulfoxide (DMSO; VWR 67-68-5) to create a 110,000 µM stock solution.

**Table 1. Molecular structure and formula of each experimental compound. Role of each compound in the study is indicated.** Chemical structure drawn in BIOVIA draw.

| Compound | Molecular Formula | Structure | Role in Study |
|---|---|---|---|
| **HP1** | $C_{10}H_{11}NO$ | 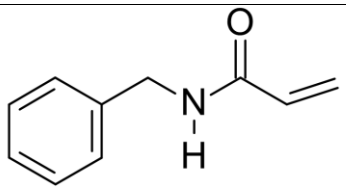 | Experimental compound with known MAF |
| **HP2** | $C_9H_9NO$ | 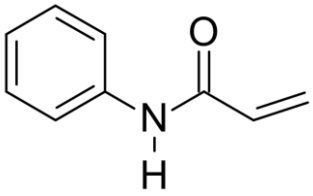 | Experimental compound with known MAF |
| **HP3** | $C_{12}H_{13}NOS$ | 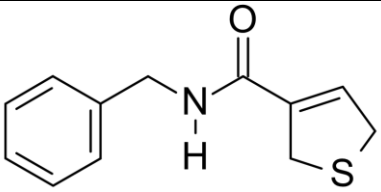 | Experimental compound with novel MAF |
| **Enone** | $C_8H_{10}OS$ | 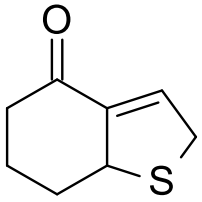 | Experimental compound from which the novel MAF was derived |
| **HP5** | $C_9H_{13}NOS$ | 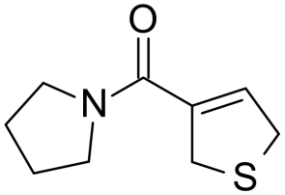 | Experimental compound with novel MAF |

### *2.2.3 Control compounds*

Cisplatin and Ibrutinib were used as control compounds for the MTT assay and cell imaging and counting. Cisplatin was dissolved in 0.9% saline solution to create a 3300 µM stock solution. Ibrutinib was dissolved in DMSO to create a 30,000 µM stock solution.

## 2.4 Treatment preparation

All treatments of the water-soluble compounds (Enone, HP1, HP2, HP5, Cisplatin) were prepared via serial dilution in complete DMEM to yield 9 final treatments at concentrations ranging from 0.5 to 316 µM.

Compounds dissolved in DMSO (Ibrutinib and HP3) were prepared by further diluting the 30,000 µM and 110,000 µM stock solutions respectively in DMSO. They were diluted into lower concentration stock solutions such that each could individually be diluted in complete DMEM to make 9 final treatments at concentrations ranging from 0.5 to 316 µM, containing 0.325% DMSO.

Final treatments for both controls were made on the day for each experiment.

## 2.5 MTT assay for cell viability

Cells were plated in a clear 96-well plate at a density of 5000 cells per well and then incubated at 37°C and 5% $CO_2$ for 24 hrs. The complete DMEM was then removed and replaced with 100 µL per well of treatments before a 48 hr incubation period at 37°C and 5% $CO_2$. 20 µL of 5 mg/ml 3-(4,5-dimethylthiazol-2-yl)-2,5-diphenyl tetrazolium bromide (MTT; VWR 298-93-1) was added to each well and the plate was incubated for another 4 hrs at 37°C and 5% $CO_2$. After this incubation, all treatment and MTT reagent were removed from the plate and replaced with 100 µL DMSO to solubilize the formazan product. The plate was protected from light with tinfoil and shaken for 10 minutes to

ensure a uniform absorbance and absorbance was measured at 570 nm using Spark Multimode Microplate Reader (Tecan, Switzerland).

**2.6 Cell morphology and cell count**

Cells were plated and treated as in the MTT Assay. After the 48 hr incubation period, 24 µL of 5 ug/ml Hoechst nuclear stain (Thermo Fisher H3570) in 16% (w/v) methanol-free paraformaldehyde (PFA) was added to each well to fix cells and stain nuclei. The plate was protected from light, then rocked for 5 minutes and left to sit at room temperature for an additional 10 minutes. The fixative and stain solution was removed and the plate washed twice with 100 µL PBS per well. 100 µL PBS was added to each well and the plate was imaged at 10X magnification using ImageXpress Pico Automated Cell Imaging system (Molecular Devices, USA). Brightfield images were captured to assess cell morphology. Fluorescent images of Hoechst stained nuclei were captured through the DAPI (370/450 nm) filter to assess nuclei morphology and allow for cell counting. After image acquisition, Cell Reporter Xpress software (Molecular Devices, USA) automated cell count protocol was used to count cells.

**2.7 Data analysis**

GraphPad Prism 10 software (GraphPad) was used for all statistical analysis and to generate all graphs. MTT assay spectrophotometric data was adjusted to the average of the blanks and then % viability was calculated as absorbance value of wells with cells treated with compounds relative to that of the negative control (untreated cells). The concentrations were log transformed in GraphPad Prism 10 before the data was graphed in the software. To graph the dose-response curves, the MTT assay data was fit to the log[inhibitor] vs response model, the mean of each treatment was plotted with error bars as standard error of the mean (SEM). To calculate the IC50 values MTT assay data

was fit to the log [inhibitor] vs normalized response model, the concentrations were log transformed in the same way.

Cell count data was normalized to the negative control (untreated cells), for each trial cell count data was divided by the average number of cells counted in the negative control condition. The Shapiro-Wilks test was used to confirm normal distribution of the data prior to the ANOVA. A Brown-Forsythe test for equal variance was also conducted prior to the ANOVA. The data did not pass the assumption of equal variance so a Brown-Forsythe one-way ANOVA was conducted. Dunnett's T3 multiple comparison test was then used to determine significant differences between cell count. The significance level chosen for statistical analysis was $p < 0.05$.

# 3. Results

## 3.1 Treatment concentration optimization

Cisplatin was the initial positive control used in this study. Consequently, the treatment concentrations of the experimental compounds tested were in the same range as Cisplatin. It was found that 48 hrs of exposure to 316 µM Cisplatin was adequate to induce approximately 100% cell death. Thus, the concentration range for all experimental treatments and Cisplatin was 0 to 316 µM. A Michael acceptor positive control, Ibrutinib, was acquired later in the project. It was found that 30 µM Ibrutinib was adequate to induce approximately 100% cell death after 48 hrs of exposure.

## 3.2 MTT assay

MTT assays were conducted to evaluate how cytotoxicity varied between experimental compounds and doses, using cellular metabolism as a proxy. The dose-response relationship of each compound and maximum effect on cell viability (Emax) appeared to vary between all compounds. The Emax is the bottom plateau of the graph, it shows the "maximal effect on viability at maximum treatment concentration" (Larsson et al., 2020). The Emax of the novel Michael Acceptors (HP3 and HP5) appeared to fall between that of the known Michal Acceptors (HP1 and HP2) although poor fit of the data to the model (**Table 2**) prevented the determination of exact Emax values within a reasonable confidence interval (**Table 2**). The Emax of the Enone (**Table 2**) was comparable to that of Cisplatin and Ibrutinib and caused around 100% cell death.

The overall slopes of HP1, HP2, HP3, and HP5 descended gradually and consistently (**Figure 4**), revealing what appeared to be a fairly linear relationship with dose within the concentration range tested. HP2 does exhibit a sharp drop in cell viability at the highest concentration. This may explain the particularly poor fit of these compounds to the model as it assumes a sigmoidal relationship between dose and response (Motulsky, n.d.). The sigmoidal relationship is assumed because most dose-

response models follow the receptor binding curve shape where between maximum and minimum response there is a steep change in response (Motulsky, n.d.). The steep change in response is measured as the Hill Slope (slope factor) and a Hill slope of -1.0 represents the slope of a standard inhibition dose-response curve (Motulsky, n.d.). The Enone curve has the classic sigmoidal shape seen in most dose response curves and has a hill slope near -1.0 (Hill Slope = -1.293).

The half-maximal inhibitory concentration (IC50) of the Enone (IC50 = 11.56 µM) was very close to that of Cisplatin (IC50 = 12.19 µM), further highlighting the high toxicity of this compound. The IC50 of Ibrutinib (IC50 = 0.09111 µM) was found to be more than 100 fold smaller than that of the Enone or Cisplatin, demonstrating that it is extremely toxic to HCT116 cells at low concentrations. Ibrutinib is presented on a separate graph (**Figure 4**) because the concentration range tested (0-30 µM) was an order of magnitude different from that of the other compounds (0-316 µM). The IC50 values of HP1 and HP5 could not be accurately determined as they never reduced cell viability below 50%. Regarding HP2 and HP3, the IC50 values could not be accurately determined as they did not sufficiently reduce cell viability below 50%. Poor fit to the model (**Table 3**) hindered accurate IC50 calculation in these cases.

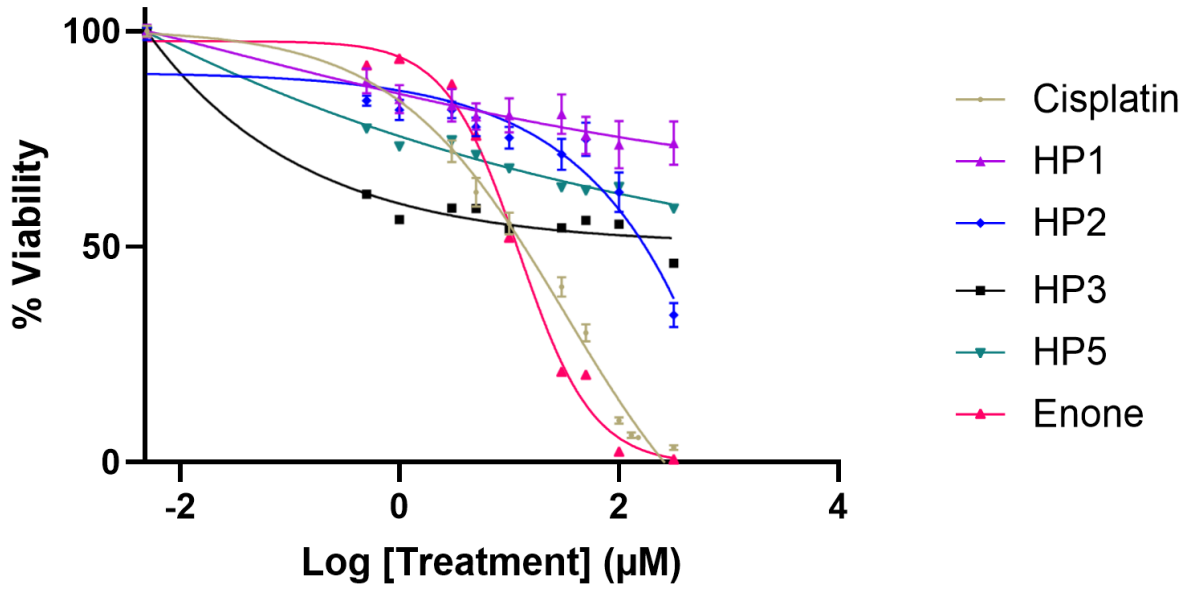


**Figure 4. MTT assay measuring cellular metabolism as a proxy for cell viability**. Percentage viability of HCT116 cells after 48 hours of exposure to experimental treatments and positive control Cisplatin. Percentage viability of each treatment was normalized to the zero treatment condition. The data points are presented as mean ± SEM. Error bars not shown when smaller than the symbols. (experimental treatments: n= 15 per concentration, Cisplatin: n=20). Data was plotted using the "log[inhibitor] vs. response – Variable slope" model in GraphPad Prism 10. Model parameters are presented in **Table 2**.

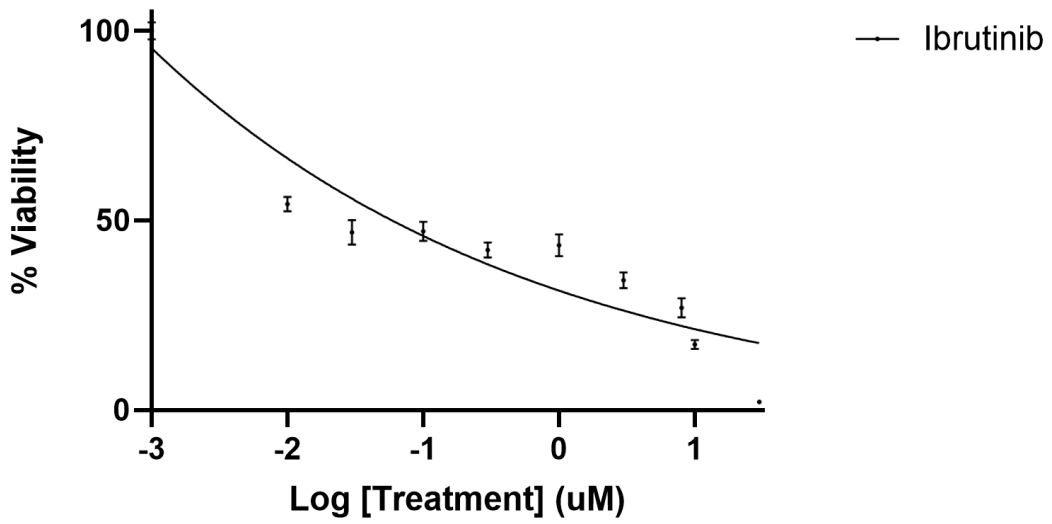


**Figure 5 MTT assay measuring cellular metabolism as a proxy for cell viability**. Percentage viability of HCT116 cells after 48 hours of exposure to positive control Ibrutinib. Percentage viability of each was normalized to the zero treatment condition. The data points are presented as mean ± SEM. Error bars not shown when smaller than the symbols. (n=10 per concentration). Data was plotted using the "log[inhibitor] vs. response – Variable slope" model in GraphPad Prism 10. Model parameters are presented in **Table 2** except for IC50 (half-maximal inhibitory concentration) which is presented in **Table 3**.

**Table 2. Hill Slope and Emax values calculated by "log[inhibitor] vs. response – Variable slope" model.** Hill Slope and Emax are shown for compounds that fit the model well enough to produce values with a reasonable 95% confidence interval. (Experimental treatments: n= 15, Cisplatin: n=20, Ibrutinib: n=10). This model does not constrain Y values and is more representative of Hill Slope and Emax. The model was run in GraphPad Prism 10.

| Compound | **Hill Slope** | 95% Confidence Interval | **Emax (%Viability)** | 95% Confidence Interval | **$R^2$ (Goodness of fit)** |
|---|---|---|---|---|---|
| Ibrutinib | -0.1579 | -0.2318, -0.07840 | -1.224 | -56.30, 15.49 | 0.8120 |
| Cisplatin | -0.5567 | -0.6692, -0.4602 | -31.49 | -59.83, -16.48 | 0.9337 |
| Enone | -1.293 | -1.531, -1.098 | -0.4737 | -5.717, 4.087 | 0.9498 |
| HP3 | - | - | - | - | 0.4156 |
| HP5 | - | - | - | - | 0.4132 |
| HP1 | - | - | - | - | 0.1951 |
| HP2 | - | - | - | - | 0.6442 |

**Table 3. IC50 (half-maximal inhibitory concentration) values calculated by "log[inhibitor] vs. normalized response – Variable slope" model.** IC50 values are shown for compounds that fit the model well enough to produce IC50 values with a reasonable 95% confidence interval.(Experimental treatments: n= 15, Cisplatin: n=20, Ibrutinib: n=10). This model forces Y values to run from 100 down to 0 and produces more accurate IC50 values. The model was run in GraphPad Prism 10.

| Compound | **IC50 (μM)** | 95% Confidence Interval | **$R^2$ (Goodness of fit)** |
|---|---|---|---|
| Ibrutinib | 0.09111 | 0.05865, 0.1387 | 0.7539 |
| Cisplatin | 12.19 | 10.90, 13.59 | 0.9204 |
| Enone | 11.56 | 10.59, 12.63 | 0.9490 |
| HP3 | - | - | -3.548 |
| HP5 | - | - | - |
| HP1 | - | - | 0.1867 |
| HP2 | - | - | 0.5962 |

### *3.3 Cell counting*

Cell counting was done to evaluate viability of HCT116 cells after 48 hours of exposure to the highest concentration of the experimental treatments (316 μM). The cell count data supports the trend seen in the dose-response curves (**Figure 4**) that shows the Enone appeared to have much lower value for Emax (i.e. results in lower cell viability) compared to the other experimental compounds. Although, Emax could not be generated for every compound, comparison of cell count after 48 hours between each experimental treatment correlated with the in Emax values qualitatively observed from the dose response curves, i.e. the end point of the curves (**Figure 4**). That is, the order of cytotoxicity of experimental compounds as qualitatively observed in **Figure 4** is reflected in cell count data which statistically shows there is a significant difference in reduction of cell viability between all experimental compounds (**Table A1**). HP1 is the only compound that does not induce significant cell death relative to the negative control (p= 0.1573). Panel A in **Figure 7** provides a qualitative view of the reduction of viable cells.

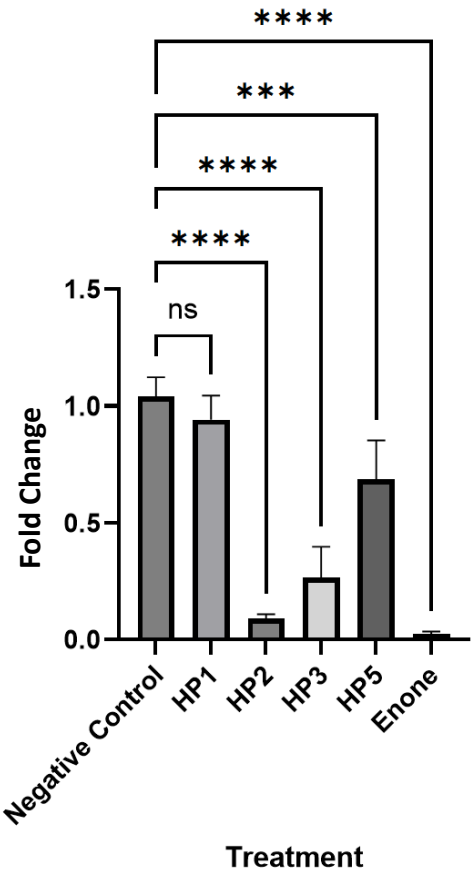


**Figure 6. HCT116 cell count.** Cell count after 48 hours of exposure to highest concentration of treatments (316 µM). Data normalized to negative control (zero treatment). (n=10 per treatment). Statistically significant differences determined with Dunnnett's T3 multiple comparisons test post Brown-Forsythe one-way ANOVA. Significant difference from negative control marked with *** ($p<0.0002$), **** ($p< 0.0001$). No significant difference marked with "ns" ($p = 0.1456$). GraphPad Prism 10 used for graph generation and statistical analysis.

### 3.4 Morphological analysis of cell death pathway

The type of cell death occurring after each treatment was assessed by visually analyzing the morphology of HCT116 cells in both brightfield and fluorescent images (DAPI). The images taken were of cells exposed to the highest concentration of the treatments for 48 hrs. In **Figure 7**, the morphology of healthy HCT116 cells can be seen under the negative control (zero treatment). The majority of these cells were adhered to the plate and had a number of projections stretching from the cell body

(pseudopodium). The cells also exhibited typical, undistorted membrane structure as well as typical nuclear shape and size.

### *3.4.1 Apoptotic morphologies*

HCT116 Cells exposed to the highest concentrations of Cisplatin, Ibrutinib, Enone, HP1, and HP2, for 48 hrs exhibited morphologies characteristic of apoptosis. Almost all of the cells that remained after exposure to Cisplatin, Ibrutinib, Enone, or HP2 had shrunken and become round. This indicates that that they retracted their pseudopodia and detached from the cell culture plate. The fewer number of cells, of which many are fragmented, suggests that late-stage apoptosis is occurring in cells exposed to Cisplatin, Ibrutinib, and Enone. Pyknosis, another characteristic of apoptosis, coincided with the cell rounding and shrinkage. It is visible in the DAPI images as brighter and smaller nuclei. These nuclei are brighter because pyknosis is occurring and consequently the DNA specific fluorescent dye is concentrated. HCT116 cells exposed to HP1 exhibited these same morphological changes in some cells, however, in contrast to the other treatments many more cells were present and the majority of them had the same healthy morphology observed in the negative control.

### *3.4.2 Necrotic morphologies*

HCT116 cells exposed to the highest concentration of HP3 and HP5 for 48hrs exhibited morphologies consistent with both apoptosis and necrosis. There was some cell rounding and pyknosis visible which is indicative of apoptosis. The majority of the cells exposed to these treatments exhibited what appeared to be necrotic morphologies. Most evidently these cells were seen to have swollen to a much larger size compare to the healthy negative control cells. Complimentary to the swelling, these cells appeared to have lost their membrane integrity which was evident by the membrane rupturing. In contrast to apoptotic cells, these cells remained attached to the plate and although

disfigured by swelling, retained resemblance to the polygonal shape of the healthy control cells instead of becoming shrunken and rounded. In DAPI images of the stained HCT116 nuclei (**Figure 7 panel B**) it can be seen that the nuclei of the swollen cells were of similar size and brightness to that of the healthy control cells. This indicates that pyknosis was not occurring.

A conspicuous morphological difference separating the necrotic cells from the healthy negative control cells and apoptotic cells was the ubiquitous presence of white dots as observed in the brightfield images (**Figure 7**). These white dots may be autophagosomes (autophagic vacuoles) or autolysosomes. Rather than being its own category of cell death, autophagy is often a mechanism by which cells attempt to rescue themselves from necrosis or apoptosis (Kroemer et al., 2009). Autophagy has two potential, additional roles that complement the finding that these cells were dying via necrosis rather than contradict it. Autophagy may aid in initiating necrosis and is important in the clean up process by degrading cell components and signaling for phagocytes to remove cell debris (Kroemer & Levine, 2008).

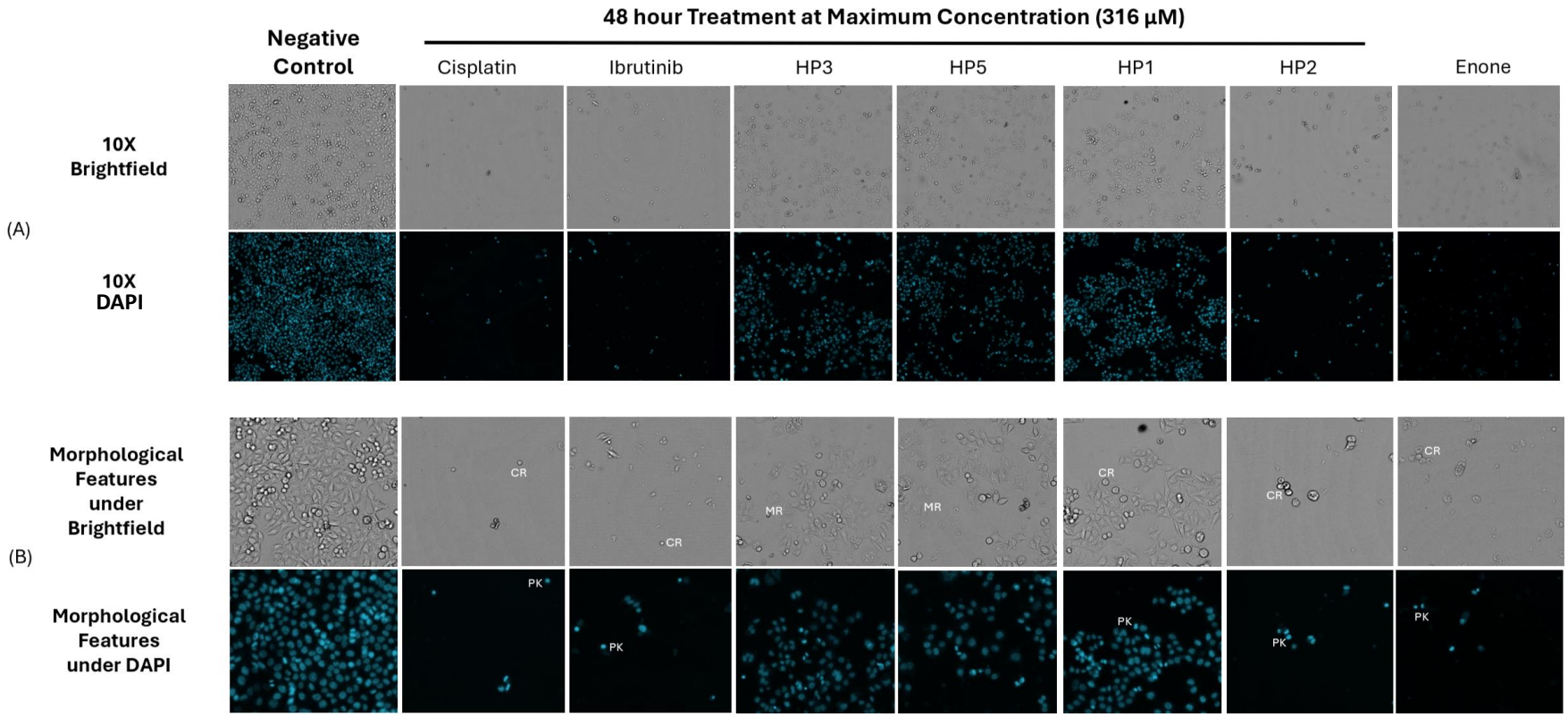


**Figure 7. Images of HCT116 cells after 48 hours of exposure to highest concentration of treatments (316 µM).** Images were captured at 10X magnification for brightfield and fluorescent DAPI images. Brightfield images were captured under standard transmitted light microscopy and DAPI images were captured under fluorescent imaging with the DAPI (370/450 nm) filter. DAPI images show Hoescht-stained nuclei of cells. Images in panel A are representative of reduction in cell viability after each treatment. Images in Panel B have been enlarged to showcase morphological changes post treatment exposure. (MR = Membrane rupture, PK= pyknosis, CR= Cell rounding). Images were taken on ImageXpress Pico Automated Cell Imaging system (Molecular Devices, USA).

# 4. Discussion

MACs have the potential to act as powerful irreversible enzyme inhibitors due to their unique Michael acceptor chemistry that allows them to form strong covalent bonds with targets within enzyme active sites (Jackson et al., 2017). This is particularly beneficial when it comes to hard-to-target, shallow bindings sites in enzymes and can be a mechanism of overcoming resistance in certain cancers (Jackson et al., 2017). Cancer resistance to chemotherapy treatments can develop in a wide variety of ways rendering some of the current therapeutics ineffective (Mansoori et al., 2017). It is important to continue to explore avenues for developing novel chemotherapeutics to counter this resistance. Therefore, this study explored the cytotoxicity and cell death pathway induced by compounds with a novel MAF (novel MACs) in HCT116 cells. Cytotoxicity was investigated using cell count and the MTT assay which uses cellular metabolism as a proxy for cell viability. Cell and nuclear morphology were analyzed in brightfield and fluorescent DAPI images to begin to determine the cell death pathway being initiated. The MAF developed for this study can be added to a variety of backbone molecules containing primary or secondary amines and thus may provide the foundation for the development of novel chemotherapeutics when future research identifies or designs the optimal backbone structures for selectivity.

## 4.1 Cytotoxicity induced in HCT116 cells

The findings of the cytotoxicity measurements in this study support our **hypothesis that the MACs would exhibit varying degrees of cytotoxicity depending on molecular structure**. The MTT assay provided insight into the varying dose-response profiles of the treatments in this study i.e. how an increase in dose affects the level of cytotoxicity of the compounds. Many of the MACs didn't exhibit a classic dose-response shaped curve within the concentration range tested as they did not induce sufficient cytotoxicity, and thus some parameters such as Emax could not be accurately estimated

by the model. In place of this, the cell count data provided further insight into the cytotoxicity of the MACs at their highest concentration.

### *4.1.1 Cytotoxicity of the novel Michael acceptors*

Both of the novel MACs HP3 and HP5 were able to induce a significant amount of cell death relative to the negative control as was measured by cell count. This shows that these novel MACs are cytotoxic towards HCT116 cells. The results from the MTT assay showed that there was a fairly gradual decrease in cell viability as dose increased. It was observed from both cell count and MTT assay, that the maximum concentration of these compounds induced cytotoxicity that falls between that of the known MACs HP1 and HP2.

Between the two novel Michael acceptor compounds HP5 was significantly less cytotoxic than HP3. One explanation for this finding is that it is possible that the MAF position on HP5 exists not as shown in **Table 1**, it may exist in a position that is less favourable for the MAR to occur. Assessing the Michael acceptor reactivity (i.e. ability to undergo Michael addition) of these compounds through experiments such as reaction kinetics analysis and computational modeling would be useful next steps for determining if this is the case and if the Michael acceptor reactivity varies between these two compounds (Huang et al., 2021). Furthermore, the chemical backbones of these compounds were not designed to target specific sites within the cell and thus it cannot be ruled out that this difference had some level of impact on cytotoxicity.

The MAF on the compounds HP3 and HP5 were developed from the known MAC called the Enone. This compound caused around 100% cell death at the maximum concentration tested and had an IC50 very similar to that of the chemotherapy drug positive control Cisplatin. This suggests that a MAF developed from the Enone has the potential to induce cytotoxicity levels similar to current chemotherapy drugs depending on the chemical backbone attached. The Enone may also have such potent toxicity partly

due to its small size as small molecules can more readily passively diffuse into cells (Yang & Hinner, 2015).

The positive control Michael acceptor drug, Ibrutinib, was found to be far more toxic than any of the other compounds as indicated by its IC50 value. There is evidence that Ibrutinib can target kinases other than BTK in malignant B-cells (Berglöf et al., 2015). This may explain the potent cytotoxicity observed in HCT116 cells in this study.

## 4.2 Cell death pathway

### *4.2.1 Novel Michael acceptor compounds may induce necrosis in HCT116 cells*

Upon exposure to the highest concentration of novel treatments (HP3 and HP5), the majority of HCT116 cells appeared to be undergoing cell death via necrosis. Morphological markers in brightfield images suggested the occurrence of necrosis and this was supported by nuclear morphology observed in fluorescent DAPI images. Necrosis involves cellular swelling and membrane rupture followed by uncontrolled loss of intracellular contents (Kroemer et al., 2009). The markers of necrotic cell death coincided with the presence of what appeared to be autophagosomes. This is consistent with previous studies that have found that α,β-unsaturated ketones, a MAC, are capable of inducing non-apoptotic cell death paired with presence of autophagosomes (Sakagami et al., 2007).

Tumour necrosis has typically been associated with poor prognosis for patients (Richards et al., 2011). As a result of their rapid growth that outpaces the blood supply available, the center of tumours can lack adequate oxygen and nutrient supply (Yee & Li, 2021). This can lead to hypoxia-induced, glucose deprivation-induced, or ROS-induced cell death, that often occurs via the necrosis cell death pathway (Yee & Li, 2021). Some studies suggests that tumour cells dying by necrosis release proteins that promote invasion and metastasis (Liu & Jiao, 2020). However, despite being associated with aggressive tumour growth and metastasis, the exact ways in which necrosis is implicated remains unresolved (Liu & Jiao, 2020). Research into the relationship between necrosis

and tumor progression is ongoing, and there is a growing body of research that suggests that inducing sub-types of necrosis cell death provide a mechanism for overcoming cancer drug-resistance (Yu et al., 2020).

Necroptosis, also known as regulated necrosis, is a subtype of necrosis (Berghe et al., 2010). It is considered a programmed type of necrosis that is genetically and biochemically distinct but morphologically almost identical (Berghe et al., 2010). Compounds that induce the necroptosis cell death pathway are of interest in the development of novel chemotherapeutics as apoptosis suppression is a major mechanism of anticancer drug resistance (Mansoori et al., 2017). In addition to triggering a cell death pathway other than apoptosis, there is a growing body of research showing that necroptosis is capable of inducing anti-tumour immunity to some degree (Krysko et al., 2017). An increase in anti-tumour ability describes an increase in immune system activity against the tumour such that it is better controlled (Ramella & Postow, 2016). In a study by Aaes et al., it was found that necroptotic cancer cells were very efficient in inducing anti-tumor immunity (Aaes et al., 2016). They found that necroptotic cells release death related molecules called Damage-associated molecular patterns (DAMPs) which in turn promote the maturation of antigen presenting dendritic cells (Aaes et al., 2016). This led to the effective cross-priming of white blood cells (CD8a+ T cells) i.e. effective presentation of the tumor antigens to the white blood cells, leading to a tumor specific immune response (Aaes et al., 2016). Overall, anti-tumour immunity is a powerful tool to fight cancer and has a significant impact on patient prognosis (YOSHIMOTO et al., 2015).

It is likely that necrosis and its subtypes play both a positive and negative role in tumour development (Liu & Jiao, 2020). As we gain a deeper understanding into the mechanisms by which they can promote or inhibit tumour progression, the nuances of the pathways, and their relationship to different stages of tumorigenesis (Liu & Jiao, 2020), it will become more clear how and when the power of necrosis-inducing drugs should be harnessed in the fight against cancer.

### *4.2.2 Known Michael acceptor compounds may induce apoptosis in HCT116 cells*

In contrast, the experimental known MACs (HP1, HP2 and Enone) along with positive control Cisplatin and Ibrutinib appeared to induce apoptosis in HCT116 cells. Whole cell morphology in brightfield images and nuclear morphology in fluorescent DAPI images were consistent with apoptotic morphological changes. What determines which cell death pathway cells die by is extremely complicated and requires extensive investigation into the cell death signalling (Green & Llambi, 2015). Thus, it is not currently known why these MACs appear to have induced apoptosis. As previously discussed, apoptosis suppression is a mechanism cancer cells may use to resist anticancer drugs (Mansoori et al., 2017). In future studies it would be interesting to investigate if these compounds can consistently induce apoptosis in cancer cells despite apoptosis avoidance mechanisms. A previous study by Kühn et al. found that certain nitro-fatty acids, lipids with a MAF, were able to induce apoptosis in HCT116 cells (Kühn et al., 2018).

Analysis of cell death using morphological analysis of cells under brightfield microscopy and morphological analysis of fluorescent stained nuclei provide a quick way to examine cell death (Galluzzi et al., 2009). However, morphological analysis in this manner alone is insufficient to concretely determine cell death pathway (Galluzzi et al., 2009). It is therefore suggested that biochemical assays for apoptosis and necrosis should be conducted to confirm the morphological analysis.

## 4.3 Conclusion and future directions

This explorative study shows that the novel MACs are capable of inducing cytotoxicity against HCT116 cancer cells. Along with the potent toxicity of the Enone, these results warrant further investigation into the cytotoxicity of the novel MAF against various cancer cell lines. Future studies should investigate whether replacing the current MAFs on anticancer drugs with the novel MAF can increase the effectiveness of these drugs.

## 5. References


Aaes, T. L., Kaczmarek, A., Delvaeye, T., De Craene, B., De Koker, S., Heyndrickx, L., Delrue, I., Taminau, J., Wiernicki, B., De Groote, P., Garg, A. D., Leybaert, L., Grooten, J., Bertrand, M. J. M., Agostinis, P., Berx, G., Declercq, W., Vandenabeele, P., & Krysko, D. V. (2016). Vaccination with Necroptotic Cancer Cells Induces Efficient Anti-tumor Immunity. *Cell Reports*, *15*(2), 274–287. https://doi.org/10.1016/j.celrep.2016.03.037

Arnason, J. E., & Brown, J. R. (2017). Targeting B Cell Signaling in Chronic Lymphocytic Leukemia. *Current Oncology Reports*, *19*(9), 61. https://doi.org/10.1007/s11912-017-0620-7

Berghe, T. V., Vanlangenakker, N., Parthoens, E., Deckers, W., Devos, M., Festjens, N., Guerin, C. J., Brunk, U. T., Declercq, W., & Vandenabeele, P. (2010). Necroptosis, necrosis and secondary necrosis converge on similar cellular disintegration features. *Cell Death & Differentiation*, *17*(6), Article 6. https://doi.org/10.1038/cdd.2009.184

Berglöf, A., Hamasy, A., Meinke, S., Palma, M., Krstic, A., Månsson, R., Kimby, E., Österborg, A., & Smith, C. I. E. (2015). Targets for Ibrutinib Beyond B Cell Malignancies. *Scandinavian Journal of Immunology*, *82*(3), 208–217. https://doi.org/10.1111/sji.12333

Boike, L., Henning, N. J., & Nomura, D. K. (2022). Advances in covalent drug discovery. *Nature Reviews Drug Discovery*, *21*(12), Article 12. https://doi.org/10.1038/s41573-022-00542-z

Burger, J. A., & Chiorazzi, N. (2013). B cell receptor signaling in chronic lymphocytic leukemia. *Trends in Immunology*, *34*(12), 592–601. https://doi.org/10.1016/j.it.2013.07.002

Evans, D. C., Watt, A. P., Nicoll-Griffith, D. A., & Baillie, T. A. (2004). Drug−Protein Adducts: An Industry Perspective on Minimizing the Potential for Drug Bioactivation in Drug Discovery and Development. *Chemical Research in Toxicology*, *17*(1), 3–16. https://doi.org/10.1021/tx034170b

Galluzzi, L., Aaronson, S. A., Abrams, J., Alnemri, E. S., Andrews, D. W., Baehrecke, E. H., Bazan, N. G., Blagosklonny, M. V., Blomgren, K., Borner, C., Bredesen, D. E., Brenner, C., Castedo, M., Cidlowski, J. A., Ciechanover, A., Cohen, G. M., De Laurenzi, V., De Maria, R., Deshmukh, M., … Kroemer, G. (2009). Guidelines for the use and interpretation of assays for monitoring cell death in higher eukaryotes. *Cell Death & Differentiation*, *16*(8), 1093–1107. https://doi.org/10.1038/cdd.2009.44

Ghasemi, M., Turnbull, T., Sebastian, S., & Kempson, I. (2021). The MTT Assay: Utility, Limitations, Pitfalls, and Interpretation in Bulk and Single-Cell Analysis. *International Journal of Molecular Sciences*, *22*(23), 12827. https://doi.org/10.3390/ijms222312827

Ghia, P., Ferreri, A. J. M., & Caligaris-Cappio, F. (2007). Chronic lymphocytic leukemia. *Critical Reviews in Oncology/Hematology*, *64*(3), 234–246. https://doi.org/10.1016/j.critrevonc.2007.04.008

González-Bello, C. (2016). Designing Irreversible Inhibitors—Worth the Effort? *ChemMedChem*, *11*(1), 22–30. https://doi.org/10.1002/cmdc.201500469

Green, D. R., & Llambi, F. (2015). Cell Death Signaling. *Cold Spring Harbor Perspectives in Biology*, *7*(12), a006080. https://doi.org/10.1101/cshperspect.a006080

Häcker, G. (2000). The morphology of apoptosis. *Cell and Tissue Research*, *301*(1), 5–17. https://doi.org/10.1007/s004410000193

Hanahan, D., & Weinberg, R. A. (2011). Hallmarks of Cancer: The Next Generation. *Cell*, *144*(5), 646–674. https://doi.org/10.1016/j.cell.2011.02.013

Hearn, B. R., Fontaine, S. D., Schneider, E. L., Kraemer, Y., Ashley, G. W., & Santi, D. V. (2021). Attenuation of the Reaction of Michael Acceptors with Biologically Important Nucleophiles. *Bioconjugate Chemistry*, *32*(4), 794–800. https://doi.org/10.1021/acs.bioconjchem.1c00075

Huang, S., Kim, K., Musgrave, G. M., Sharp, M., Sinha, J., Stansbury, J. W., Musgrave, C. B., & Bowman, C. N. (2021). Determining Michael Acceptor Reactivity from Kinetic, Mechanistic, and Computational Analysis for the Base-catalyzed Thiol-

Michael Reaction. *Polymer Chemistry*, *12*(25), 3619–3628. https://doi.org/10.1039/d1py00363a

Jackson, P. A., Widen, J. C., Harki, D. A., & Brummond, K. M. (2017). Covalent Modifiers: A Chemical Perspective on the Reactivity of α,β-Unsaturated Carbonyls with Thiols via Hetero-Michael Addition Reactions. *Journal of Medicinal Chemistry*, *60*(3), 839–885. https://doi.org/10.1021/acs.jmedchem.6b00788

Johnson, D. S., Weerapana, E., & Cravatt, B. F. (2010). Strategies for discovering and derisking covalent, irreversible enzyme inhibitors. *Future Medicinal Chemistry*, *2*(6), 949–964. https://doi.org/10.4155/fmc.10.21

Kroemer, G., El-Deiry, W. S., Golstein, P., Peter, M. E., Vaux, D., Vandenabeele, P., Zhivotovsky, B., Blagosklonny, M. V., Malorni, W., Knight, R. A., Piacentini, M., Nagata, S., & Melino, G. (2005). Classification of cell death: Recommendations of the Nomenclature Committee on Cell Death. *Cell Death & Differentiation*, *12*(2), Article 2. https://doi.org/10.1038/sj.cdd.4401724

Kroemer, G., Galluzzi, L., Vandenabeele, P., Abrams, J., Alnemri, E. S., Baehrecke, E. H., Blagosklonny, M. V., El-Deiry, W. S., Golstein, P., Green, D. R., Hengartner, M., Knight, R. A., Kumar, S., Lipton, S. A., Malorni, W., Nuñez, G., Peter, M. E., Tschopp, J., Yuan, J., … Melino, G. (2009). Classification of cell death: Recommendations of the Nomenclature Committee on Cell Death 2009. *Cell Death & Differentiation*, *16*(1), Article 1. https://doi.org/10.1038/cdd.2008.150

Kroemer, G., & Levine, B. (2008). Autophagic cell death: The story of a misnomer. *Nature Reviews. Molecular Cell Biology*, *9*(12), 1004–1010. https://doi.org/10.1038/nrm2527

Krysko, O., Aaes, T. L., Kagan, V. E., D'Herde, K., Bachert, C., Leybaert, L., Vandenabeele, P., & Krysko, D. V. (2017). Necroptotic cell death in anti-cancer therapy. *Immunological Reviews*, *280*(1), 207–219. https://doi.org/10.1111/imr.12583

Kühn, B., Brat, C., Fettel, J., Hellmuth, N., Maucher, I. V., Bulut, U., Hock, K. J., Grimmer, J., Manolikakes, G., Rühl, M., Kühn, A., Zacharowski, K., Matrone, C., Urbschat, A., Roos, J., Steinhilber, D., & Maier, T. J. (2018). Anti-inflammatory nitro-fatty acids

suppress tumor growth by triggering mitochondrial dysfunction and activation of the intrinsic apoptotic pathway in colorectal cancer cells. *Biochemical Pharmacology*, *155*, 48–60. https://doi.org/10.1016/j.bcp.2018.06.014

Larsson, P., Engqvist, H., Biermann, J., Werner Rönnerman, E., Forssell-Aronsson, E., Kovács, A., Karlsson, P., Helou, K., & Parris, T. Z. (2020). Optimization of cell viability assays to improve replicability and reproducibility of cancer drug sensitivity screens. *Scientific Reports*, *10*, 5798. https://doi.org/10.1038/s41598-020-62848-5

Leist, M., Single, B., Castoldi, A. F., Kühnle, S., & Nicotera, P. (1997). Intracellular Adenosine Triphosphate (ATP) Concentration: A Switch in the Decision Between Apoptosis and Necrosis. *The Journal of Experimental Medicine*, *185*(8), 1481–1486. 10.1084/jem.185.8.1481

Liang, S.-T., Chen, C., Chen, R.-X., Li, R., Chen, W.-L., Jiang, G.-H., & Du, L.-L. (2022). Michael acceptor molecules in natural products and their mechanism of action. *Frontiers in Pharmacology*, *13*. https://www.frontiersin.org/articles/10.3389/fphar.2022.1033003

Liu, Z., & Jiao, D. (2020). Necroptosis, tumor necrosis and tumorigenesis. *Cell Stress*, *4*(1), 1–8. https://doi.org/10.15698/cst2020.01.208

Mansoori, B., Mohammadi, A., Davudian, S., Shirjang, S., & Baradaran, B. (2017). The Different Mechanisms of Cancer Drug Resistance: A Brief Review. *Advanced Pharmaceutical Bulletin*, *7*(3), 339–348. https://doi.org/10.15171/apb.2017.041

Michalczyk, A., Klüter, S., Rode, H. B., Simard, J. R., Grütter, C., Rabiller, M., & Rauh, D. (2008). Structural insights into how irreversible inhibitors can overcome drug resistance in EGFR. *Bioorganic & Medicinal Chemistry*, *16*(7), 3482–3488. https://doi.org/10.1016/j.bmc.2008.02.053

Miller, M. A., & Zachary, J. F. (2017). Mechanisms and Morphology of Cellular Injury, Adaptation, and Death. *Pathologic Basis of Veterinary Disease*, 2-43.e19. https://doi.org/10.1016/B978-0-323-35775-3.00001-1

Motulsky, H. J. (n.d.). *Hill Slope*. GraphPad. https://www.graphpad.com/guides/prism/latest/curve-fitting/reg_hill_slope.htm

Piesche, M., Roos, J., Kühn, B., Fettel, J., Hellmuth, N., Brat, C., Maucher, I. V., Awad, O., Matrone, C., Comerma Steffensen, S. G., Manolikakes, G., Heinicke, U., Zacharowski, K. D., Steinhilber, D., & Maier, T. J. (2020). The Emerging Therapeutic Potential of Nitro Fatty Acids and Other Michael Acceptor-Containing Drugs for the Treatment of Inflammation and Cancer. *Frontiers in Pharmacology*, *11*. https://www.frontiersin.org/articles/10.3389/fphar.2020.01297

Ramella, M. R., & Postow, M. A. (2016). Recent advances in understanding antitumor immunity. *F1000Research*, *5*. https://doi.org/10.12688/f1000research.9356.1

Rando, R. R. (1975). Mechanisms of action of naturally occurring irreversible enzyme inhibitors. *Accounts of Chemical Research*, *8*(8), 281–288. https://doi.org/10.1021/ar50092a004

Richards, C. H., Mohammed, Z., Qayyum, T., Horgan, P. G., & McMillan, D. C. (2011). The prognostic value of histological tumor necrosis in solid organ malignant disease: A systematic review. *Future Oncology*, *7*(10), 1223–1235. https://doi.org/10.2217/fon.11.99

Riss, T. L., Moravec, R. A., Niles, A. L., Duellman, S., Benink, H. A., Worzella, T. J., & Minor, L. (2004). Cell Viability Assays. In S. Markossian, A. Grossman, K. Brimacombe, M. Arkin, D. Auld, C. Austin, J. Baell, T. D. Y. Chung, N. P. Coussens, J. L. Dahlin, V. Devanarayan, T. L. Foley, M. Glicksman, K. Gorshkov, J. V. Haas, M. D. Hall, S. Hoare, J. Inglese, P. W. Iversen, … X. Xu (Eds.), *Assay Guidance Manual*. Eli Lilly & Company and the National Center for Advancing Translational Sciences. http://www.ncbi.nlm.nih.gov/books/NBK144065/

Sakagami, H., Kawase, M., Wakabayashi, H., & Kurihara, T. (2007). Factors that Affect the Type of Cell Death Induced by Chemicals. *Autophagy*, *3*(5), 493–495. https://doi.org/10.4161/auto.4594

Shimizu, S., Yoshida, T., Tsujioka, M., & Arakawa, S. (2014). Autophagic Cell Death and Cancer. *International Journal of Molecular Sciences*, *15*(2), Article 2. https://doi.org/10.3390/ijms15023145

Sutanto, F., Konstantinidou, M., & Dömling, A. (2020). Covalent inhibitors: A rational approach to drug discovery. *RSC Medicinal Chemistry*, *11*(8), 876–884. https://doi.org/10.1039/d0md00154f

Villacorta, L., Gao, Z., Schopfer, F. J., Freeman, B. A., & Chen, Y. E. (2016). Nitro-fatty acids in cardiovascular regulation and diseases: Characteristics and molecular mechanisms. *Frontiers in Bioscience (Landmark Edition)*, *21*, 873–889. https://doi.org/10.2741/4425

Walpole, C. S. J., & Wrigglesworth, R. (1989). Enzyme inhibitors in medicine. *Natural Product Reports*, *6*(4), 311–346. https://doi.org/10.1039/NP9890600311

Wu, L., Bian, X., Kong, L., Yin, X., Mu, L., Wu, S., Gao, A., Wei, X., Guo, Z., & Ye, J. (2019). B cell receptor accessory molecule CD79 gets involved in response against Streptococcus agalactiae infection and BCR signaling in Nile tilapia (Oreochromis niloticus). *Fish & Shellfish Immunology*, *87*, 212–219. https://doi.org/10.1016/j.fsi.2019.01.012

Yang, N. J., & Hinner, M. J. (2015). Getting Across the Cell Membrane: An Overview for Small Molecules, Peptides, and Proteins. *Methods in Molecular Biology (Clifton, N.J.)*, *1266*, 29–53. https://doi.org/10.1007/978-1-4939-2272-7_3

Yee, P. P., & Li, W. (2021). Tumor necrosis: A synergistic consequence of metabolic stress and inflammation. *BioEssays : News and Reviews in Molecular, Cellular and Developmental Biology*, *43*(7), e2100029. https://doi.org/10.1002/bies.202100029

Yonekawa, T., & Thorburn, A. (2013). Autophagy and Cell Death. *Essays in Biochemistry*, *55*, 105–117. https://doi.org/10.1042/bse0550105

YOSHIMOTO, Y., KONO, K., & SUZUKI, Y. (2015). ANTI-TUMOR IMMUNE RESPONSES INDUCED BY RADIOTHERAPY: A REVIEW. *Fukushima Journal of Medical Science*, *61*(1), 13–22. https://doi.org/10.5387/fms.2015-6

Yu, J., Zhong, B., Xiao, Q., Du, L., Hou, Y., Sun, H.-S., Lu, J.-J., & Chen, X. (2020). Induction of programmed necrosis: A novel anti-cancer strategy for natural compounds.

*Pharmacology & Therapeutics*, *214*, 107593. https://doi.org/10.1016/j.pharmthera.2020.107593

Yuan, J., Shaham, S., Ledoux, S., Ellis, H. M., & Horvitz, H. R. (1993). The C. elegans cell death gene ced-3 encodes a protein similar to mammalian interleukin-1 beta-converting enzyme. *Cell*, *75*(4), 641–652. https://doi.org/10.1016/0092-8674(93)90485-9

Zhou, H., Hu, P., Yan, X., Zhang, Y., & Shi, W. (2020). Ibrutinib in Chronic Lymphocytic Leukemia: Clinical Applications, Drug Resistance, and Prospects. *OncoTargets and Therapy*, *13*, 4877–4892. https://doi.org/10.2147/OTT.S249586

## 6. Appendix

**Table A1. Results from Dunnett's T3 multiple comparisons test following Brown-Forsythe one-way ANOVA used to determine statistical significance between cell count after HCTT116 cells were exposed to the highest concentration of the treatments.**

| Treatments compared | Significant difference? | Adjusted P value |
|---|---|---|
| HP1 vs HP2 | Yes | <0.0001 |
| HP1 vs HP3 | Yes | <0.0001 |
| HP1 vs HP5 | Yes | 0.0111 |
| HP1 vs Enone | Yes | <0.0001 |
| HP2 vs HP3 | Yes | 0.0265 |
| HP2 vs HP5 | Yes | <0.0001 |
| HP2 vs Enone | Yes | <0.0001 |
| HP3 vs HP5 | Yes | 0.0001 |
| HP3 vs Enone | Yes | 0.0031 |
| HP5 vs Enone | Yes | <0.0001 |